Neutron resonance parameters of dysprosium isotopes using neutron capture yields

S. G. Shin [a], Y. U. Kye [a], G. N. Kim[c], M. W. Lee[d], Y. R. Kang[d], W. Namkung [b], and M. H. Cho [a, b*]
[a] *Department of Advanced Nuclear Engineering , POSTECH, Pohang 790-784, Korea*
[b] *Pohang Accelerator Laboratory, Pohang 790-784, Korea*
[c] *Kyungpook National University, Daegu 702-701, Korea*
[d] *Dongnam Inst. Of Radiological & Medical Science, 40 Jwadong-gil, Jangan-eup, Gijang-gun, Busan, Korea*
[*] mhcho@postech.ac.kr

1. Introduction

Dysprosium is used in the field of nuclear reactor system because it has a very large thermal neutron absorption cross-section. The dysprosium alloyed with special stainless steels is attractive for control in nuclear reactor because of the ability to absorb neutrons readily without swelling or contracting over time and its high melting point [1]. Dysprosium is also one of fission products from the thermal fission of ^{234}U, ^{233}U, and ^{239}Pu. The fission products are accumulated in the reactor core by the burn-up of the nuclear fuel and the poison effect is increased. Therefore, it is required to understand how Dysprosium as both a poison and an absorbing material in the control rod has an effect on the neutron population in a nuclear reactor system over all energy regions.

Neutron Capture experiments on Dy isotopes were performed at the electron linear accelerator (LINAC) facility of the Rensselear Polytechnic Institute (RPI) in the neutron energy region from 10 eV to 1 keV. Resonance parameters were extracted by fitting the neutron capture data using the SAMMY multilevel R-matrix Bayesian code [2].

2. Experimental Setup

The ~57 MeV electron beam which is produced by the RPI LINAC impinges on a water-cooled tantalum target while photoneutron reactions happen and pulsed neutrons are generated via the reactions. The details of the experimental conditions such as neutron targets overlap filters, pulse repetition rate, flight path length, and channel widths are listed on reference xx.. More information on the water-cooled tantalum target [3,4], the capture detector [5,6], the data acquisition system [5,7], and sample information [8] were given elsewhere.

3. Data Reduction

Data taking and data reduction technique for the experiment at the RPI LINAC are described in Reference [9]. The neutron energy at low energies which are assumed non-relativistic energy is given by

$$E_i = \frac{72.296L}{t_i - (t_0 - t_g)} \quad (1)$$

where E_i is the neutron energy in eV, L is the flight-path in m and t_i is the arrival time of the neutron and $(t_0,- t_g)$ is the time when the electron pulse impinges on the target.t0 is obtained by measuring the time gamma flash is detected. t_g is the flight time of gamma rays from the neutron target to the detector.

A minimum of 100-keV γ-energy was required in a detector segment to be counted. Data were recorded as capture events only if the total energy deposited in all 16 segments exceeded 1 MeV. The data were recorded as scattering events if the total deposited gamma-ray energy fell between 360 to 600 keV. This scattering energy region contains the 478-keV γ-ray emitted from the (n;α,γ) reaction in the $^{10}B_4C$ annular detector liner. The large amount of TOF data collected in each capture measurement was subjected to statistical integrity checks to verify the stability of the electron LINAC, the capture detector, and associated beam monitors. Any data that failed the integrity test were eliminated. Next, the data were dead-time corrected, normalized to beam monitors, and summed. The background was determined using normalized data measured with an empty aluminum can mounted on the sample changer. This background was subtracted from the normalized and summed capture spectra. The 16 individual capture spectra were then summed into a single total spectrum. Processed TOF data are expressed as capture yield. The capture yield is defined as the number of neutron captures per neutron incident on the sample. Therefore, in addition to the Dy sample data, another set of data was needed to determine the energy profile of the neutron flux. The capture yield Y_i in TOF channel i was calculated by

$$Y_i = \frac{C_i - B_i}{K\varphi_{sm,i}}, \quad (2)$$

where C_i is dead-time-corrected and monitor-normalized counting rate of the sample measurement, B_i is dead-time-corrected and monitor-normalized background counting rate, K is product of the flux normalization factor and the detector efficiency $\varphi_{sm,i}$ is smoothed, background-subtracted, and monitor-normalized neutron flux. The incident neutron flux shape was determined by mounting a 2.54-mm-thick, 97.9 wt % enriched $^{10}B_4C$ sample in the sample changer and adjusting the total energy threshold to record the

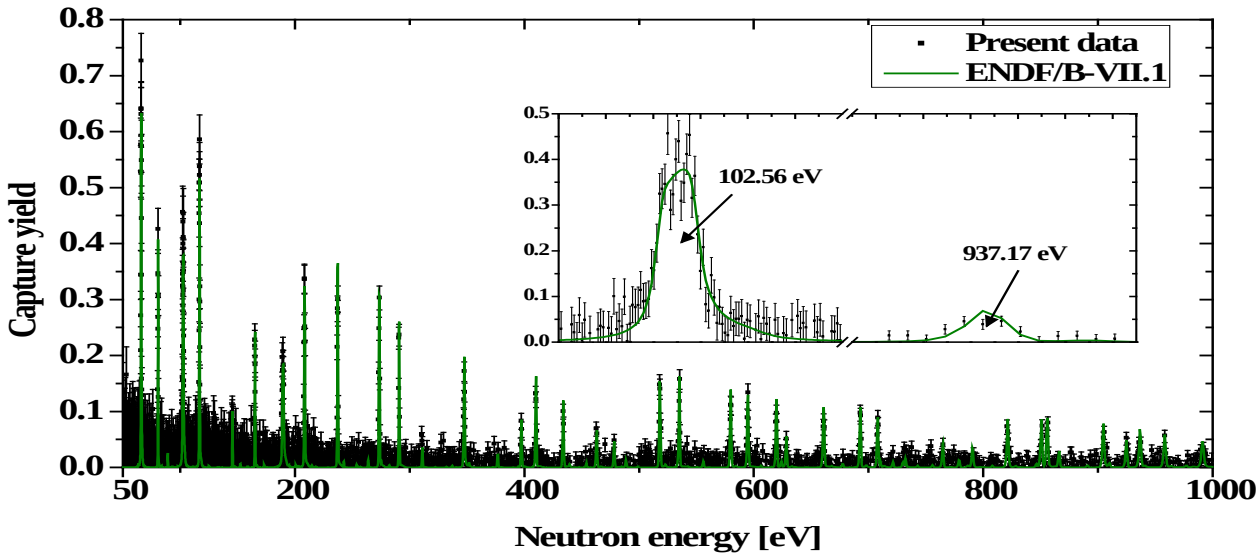

Figure 1. Capture yield data of ^{238}U and plotted curve with ENDF/B-VII.1 resonance parameters of ^{238}U.

478-keV γ-rays from neutron absorption in ^{10}B. Capture data were not used below 10 eV due to excessive background.

The resonance parameters of ^{238}U are well-known. Therefore, it is confirmed that L, t_0, and t_g in Eq. (1) are qualified by plotting the ENDF resonance parameter of ^{238}U and comparing with 20 mil ^{238}U data as shown on Figure 1.

The measured flux shape is usually normalized directly to a saturated capture resonance. However, this was not possible in this experiment because there were no saturated resonances in any of the Dy isotopes except for ^{162}Dy. The capture data were normalized using SAMMY to the 10mil natural Dy transmission data. The resonances of 18.5, 5.45, 59.06, and 147.14 eV are chosen for determining the normalization factor and detector efficiency of ^{161}Dy, ^{162}Dy, ^{163}Dy, and ^{164}Dy capture data, respectively. The transmission data was fitted at the selected resonance and the resonance parameters for normalization were obtained. In case of ^{164}Dy isotope, RPI resonance parameters were used as the initial parameters for normalization of the ^{164}Dy experimental data. The ^{nat}Dy yield data was normalized with the 18.5 eV parameters of ^{161}Dy isotope.

Table 1. The normalization factor obtained by SAMMY

Sample	Resonance Energy [eV]	Normalization factor	Normalization factor error
Natural	18.50	0.668	0.014
^{161}Dy	18.50	0.724	0.01
^{162}Dy	5.45	1.158	0.015
^{163}Dy	59.06	0.774	0.012
^{164}Dy	147.13	1.162	0.028

4. Data Analysis

Resonance parameters, neutron width Γ_n, radiation width Γ_γ, and resonance energy E_0, were extracted from the Dy capture and transmission data sets using the SAMMY multilevel R-matrix Bayesian code [2]. Dy resonance parameters and spins from the ENDF/B-VII.1 evaluation [10] were used as the initial parameters in the energy region between 10 eV to 1 keV The fitting was performed in order of transmission of natural Dy, capture yield of Dy isotope, and capture yield of natural Dy. When no further improvements in the fit were apparent, and the resonance parameters remained unchanged relative to the previous iteration, the parameters were deemed final. The SAMMY code was then used to calculate capture yield curves based on these final resonance parameters to compare with the experimental data from each Dy sample. We also examined each resonance listed in ENDF/B-VII.1 to check whether it was observed in the present data. If it did not look like a resonance peak, we removed the resonance from the parameter file.

5. Results

We observed 7, 42, and 22 new resonances not listed in ENDF/B-VII.1 from ^{160}Dy, ^{161}Dy, and ^{163}Dy isotopes, respectively as listed in Table VI. Six resonances from ^{161}Dy isotope, two resonances from ^{163}Dy, and four resonances from ^{164}Dy listed in ENDF/B-VII.1 were not observed because the present measurements did not support their existence.

The resonance integral calculations used resonance parameters from ENDF/B-VII.1 for the energy range 0 eV to 10 eV, for the negative energy resonances and for the energy region above the present measurement. The resonance integrals were calculated using the NJOY [11] and INTER [12] programs. The results are shown in Table 2 in units of barns. The uncertainty in the resonance integrals was calculated by differentiating the resonance integral with respect to resonance parameters according to the error propagation formula and treating $\sigma_\gamma(E)$ as a sum of single-level Breit-Wigner resonances

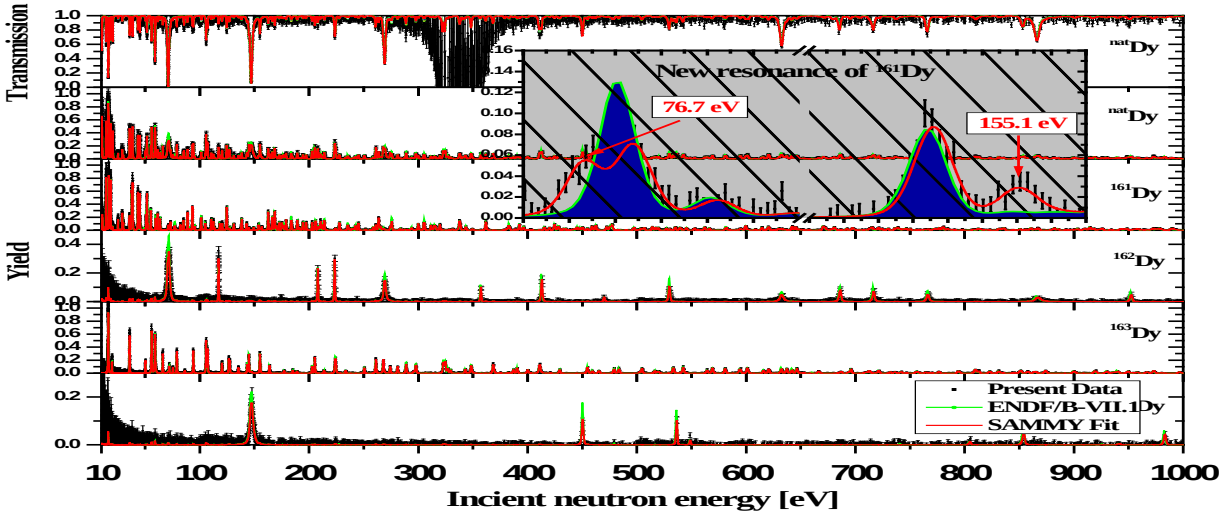

Figure 2. An overview of the present data used in the energy region.

[13]. The resonance integral of ^{160}Dy is 18.7% larger than that calculated from ENDF/B-VII.1 resonance parameters. The percent change of the resonance integral for the other isotopes are less than 3% comparing with ENDF/B-VII.1. The present parameters gave a resonance integral value of 1415±3 barn, which is ~1% higher than that obtained with the ENDF/B-VII.1 parameters.

Table 2. Calculated capture resonance integrals for dysprosium isotopes in the energy range from 0.5 eV to 20 MeV

Isotope	Abundance [%]	Capture Resonance Integral [b]		Percent Change [%]
		Present	ENDF/B-VII.1	
^{156}Dy	0.06	-	1021	-
^{158}Dy	0.1	-	247	-
^{160}Dy	2.34	1362 ± 21	1107	+ 18.7
^{161}Dy	18.9	1108 ± 13	1076	+ 2.9
^{162}Dy	25.5	2735 ± 2	2757	- 0.8
^{163}Dy	24.9	1525 ± 7	1489	+ 2.4
^{164}Dy	28.2	338.0 ± 0.6	343	- 1.5
^{nat}Dy	-	1415 ± 3	1401	+ 1

6. Conclusions

Resonance parameters were extracted from capture data sets for Dy isotopes and transmission data set of Dy natural using the multilevel R-matrix Bayesian code SAMMY. We observed 7, 42, and 22 new resonances not listed in ENDF/B-VII.1 from ^{160}Dy, ^{161}Dy, and ^{163}Dy isotopes,. Six resonances from ^{161}Dy isotope, two resonances from ^{163}Dy, and four resonances from ^{164}Dy listed in ENDF/B-VII.1 were not observed because the present measurements did not support their existence.

The capture resonance integrals were compared to resonance integrals obtained using the resonance parameters from ENDF/B-VII.1. The present parameters gave a resonance integral value of 1415±3 barn, which is ~1% higher than that obtained with the ENDF/B-VII.1 parameters.

Acknowledgment

This work is partly supported by BK21+ program through the National Research Foundation of Korea funded by the Ministry of Science, ICT & Future Planning (MSIP) (R31-30005), by the Institutional Activity Program of Korea Atomic Energy Research Institute, and by the National R&D Program through the Dong-Nam Institute of Radiological & Medical Sciences (DIRAMS) funded by MSIP (50496-2015).

REFERENCES

[1] D. R. Lide, CRC Handbook of Chemistry and Physics 88th edition, the Chemical Rubber Company (2008)

[2] N. M. Larson, Updated Users Guide for SAMMY: Multilevel R-matrix fits to Neutron Data using Bayes equations, report ORNL/TM-9179/R8 (2008)

[3] R. W. Hockenbury et al., "Neutron Radiative Capture in Na, Al, Fe, and Ni from 1 to 200 keV," Phy. Rev. 178, 4, 1746 (1969)

[4] M. E. Overberg et al., "Photoneutron Target Development for the RPI Linear Accelerator," Nucl. Instrum. Meth. A 438, 253 (1999)

[5] R. E. Slovacek et al., "Neutron Cross-Section Measurements at the Rensselaer LINAC," Proc. Topl. Mtg. Advances in Reactor Physics, April 11–15, 1994, Knoxville, Tennessee, Vol. II, p. 193, American Nuclear Society (1994)

[6] N. J. Drindak et al., "A Multiplicity Detector for Accurate Low-Energy Neutron Capture Measurements," Proc. Int. Conf. Nuclear Data for Science and Technology, May 30–June 3,1998, Mito, Japan, p. 383 (1998)

[7] R. C. Block et al., "Neutron Time-of-Flight

Measurements at the Rensselaer LINAC," Proc. Int. Conf. Nuclear Data for Science and Technology, Gatlinburg, Tennessee, May 9–13, 1994, Vol. 1, p. 81, American Nuclear Society (1994)

[8] Y. R. Kang et al., "Neutron Capture Measurements and Resonance Analysis of Dysprosium," Nuclear Data Sheets, 119, p. 162 (2014)

[9] G. Leinweber et al., "Resonance Parameters and Uncertainties Derived from Epithermal Neutron Capture and Transmission Measurements of Natural Molybdenum," Nucl. Sci. Eng. 164, 287 (2010)

[10] M B. CHADWICK et al., "ENDF/B-VII.1 nuclear data for science and technology: Cross sections, covariances, fission product yields and decay data," Nucl. Data Sheets, 112(12), 2887 (2011)

[11] R. E. MacFarlane et al., "The NJOY Nuclear Data Processing System Version 2012," LA-UR-12-27079, Los Alamos National Laboratory (2012)

[12] C. L. Dunford, "ENDF Utility Codes Release 7.01/02," USCD1212/07 (Apr. 27, 2005)

[13] D. P. Barry, "Neodymium Neutron Transmission and Capture Measurements and Development of a New Transmission Detector," PhD. Thesis, Rensselaer Polytechnic Institute (2003)